

THE PHYSICAL REVIEW

A journal of experimental and theoretical physics established by E. L. Nichols in 1893

SECOND SERIES, VOL. 127, No. 3

AUGUST 1, 1962

Magnetic Properties of He^3 at Low Temperatures*

A. C. ANDERSON, W. REESE,[†] AND J. C. WHEATLEY[‡]
Department of Physics, University of Illinois, Urbana, Illinois
(Received March 26, 1962)

The self-diffusion coefficient and the magnetic susceptibility of pure liquid He^3 have been measured, using the method of spin echoes, at pressures up to 28.2 atm and temperatures down to 0.025°K. In all cases the self-diffusion coefficient increases with decreasing temperature below 0.3°K. The temperature dependence becomes T^{-2} at the lowest temperatures, in agreement with the Landau model of a Fermi liquid. Qualitative agreement between the theoretically predicted and measured diffusion coefficients is observed over the entire range of pressures. The susceptibility is found to become independent of temperature at sufficiently low temperatures, except possibly at the highest pressures, in agreement with the Fermi liquid theory. The susceptibility divided by the density was found to increase monotonically with pressure.

INTRODUCTION

THE first experiments which demonstrated unusual magnetic properties in He^3 were performed by Fairbank and co-workers¹ who reached a low temperature of somewhat above 0.1°K. At this temperature, the susceptibility of the He^3 , at least at low pressures, was nearly independent of temperature, a result consistent with the behavior of He^3 as a Fermi liquid.² The magnitude of the susceptibility indicated that, whereas the Fermi statistics favored antiparallel alignment for the nuclear spins, the effective spin-dependent interactions favored parallel alignment; the over-all effect being to increase the susceptibility substantially over the value expected for a gas of weakly interacting atoms. The measurements were made using steady-state nuclear resonance techniques, sweeping through the resonance, broadened by field inhomogeneities much more than the natural linewidth, and observing the height of the resonance on an oscilloscope.

More recently, the method of spin echoes was applied to the problem of He^3 by Garwin and Reich³, who meas-

ured the magnetization self-diffusion coefficient, D , and the nuclear spin-lattice relaxation time, T_1 . Although their experiments were carried to a low temperature of 0.5°K, they found that D , even at low pressure, continued to decrease as the temperature, T , decreased, D becoming nearly temperature independent near 0.5°K. The self-diffusion coefficient was measured down to 0.07°K at low pressures by Hart and Wheatley⁴ also using the method of spin echoes. These authors found a remarkable increase in D as T decreased below 0.5°K, an effect to be expected for a Fermi liquid. The diffusion coefficient measured in reference 4 had a T^{-3} temperature dependence at low temperatures rather than the T^{-2} temperature dependence expected from qualitative considerations.

In a second experiment,⁵ carried to a temperature of 0.03°K, the temperature dependence $T^{-\frac{1}{2}}$ was again observed, although in this experiment probable systematic errors of $\pm 5\%$ existed as a result of spurious susceptibilities in materials used for construction. The susceptibility at low T was also measured, the result being in agreement with a reasonable extrapolation of the data in reference 1. In a third experiment,⁶ performed under better conditions with much improved techniques, and carried to 0.02°K, the temperature dependence of D below 0.04°K was found to be T^{-2} in agreement with the qualitative notions of the Fermi

* This work has been supported by the U. S. Atomic Energy Commission and the Alfred P. Sloan Foundation. It is being submitted by W. Reese in partial fulfillment of the requirement for the Ph.D. degree at the University of Illinois.

[†] National Science Foundation Fellow.

[‡] A. P. Sloan Fellow.

¹ W. M. Fairbank, W. B. Ard, and G. K. Walters, *Phys. Rev.* **95**, 566 (1954). W. M. Fairbank and G. K. Walters, *Proceedings of the Symposium on Solid and Liquid Helium Three* (Ohio State University Press, Columbus, Ohio, 1958), p. 220.

² L. D. Landau, *J. Exptl. Theoret. Phys.* (U.S.S.R.) **30**, 1058 (1956) [English translation: *Soviet Phys.—JETP* **3**, 920 (1957)].

³ R. L. Garwin and H. A. Reich, *Phys. Rev.* **115**, 1478 (1959).

⁴ H. R. Hart and J. C. Wheatley, *Phys. Rev. Letters* **4**, 1 (1960).

⁵ A. C. Anderson, H. R. Hart, and J. C. Wheatley, *Phys. Rev. Letters* **5**, 133 (1960).

⁶ A. C. Anderson, W. Reese, R. Sarwinski, and J. C. Wheatley, *Phys. Rev. Letters* **7**, 220 (1961).

liquid theory and with the results of recent experiments on specific heat,⁷ thermal conductivity,⁸ and sound propagation⁹ in liquid He³ at low pressures. The susceptibility below 0.1°K as measured in reference 6 was in excellent agreement with that obtained with different apparatus in reference 5.

In the measurements described in this paper we have repeated the low-pressure work and have extended the measurements to higher pressure in order to make a systematic study of the effect of pressure.

THEORY

The theory of a Fermi liquid was developed by Landau^{2,10,11} and later amplified by Abrikosov and Khalatnikov¹² and Hone.¹³ Within the framework of this theory, which is essentially phenomenological in nature, He³ is thought of as a gas of weakly interacting quasi-particles which move in a self-consistent field due to the other particles. The distribution function for the quasi-particles has the same form as the conventional Fermi function for a gas of free particles, but the energy of a quasi-particle is a functional of the distribution function. The theory is expected to be valid only if the quasi-particle states are well defined, that is, if the broadening \hbar/τ of quasi-particle states due to collisions of frequency $1/\tau$ is much less than kT . As a result of excessive collision rates the theory is not expected to be valid above some temperature region, but the theory does not predict this temperature region. Among other results the theory predicts a specific heat linear in temperature with coefficient proportional to the quasi-particle effective mass, a temperature-independent susceptibility and sound velocity, and a quasi-particle collision time proportional to T^{-2} . Using the theories of Abrikosov and Khalatnikov¹² and Hone¹³ and the method of evaluating quasi-particle scattering probabilities suggested by Landau,¹¹ it is possible¹⁴ to relate the transport properties (diffusion coefficient, viscosity, and thermal conductivity) to parameters derived from measurements of the specific heat, velocity of sound, susceptibility, and density. In this way it is possible to obtain a semiquantitative check on the internal consistency of the theory.

In our apparatus we measure the nuclear susceptibility relative to its value at temperatures near 1°K

and also the self-diffusion coefficient for the nuclear magnetization. According to the Landau theory,² the susceptibility at low temperatures can be written

$$\chi = \frac{1}{4}\gamma^2\hbar^2(\partial\tau/\partial\epsilon)_\mu[1 + \frac{1}{4}\bar{\xi}(\partial\tau/\partial\epsilon)_\mu]^{-1}, \quad (1)$$

where γ is the gyromagnetic ratio (2.038×10^4 G⁻¹ sec⁻¹ for He³), \hbar is Planck's constant divided by 2π , $(\partial\tau/\partial\epsilon)_\mu$ is the number of states per unit energy range and per unit volume at Fermi surface, and $\bar{\xi}$ is the average over the Fermi surface of the spin-dependent portion of the phenomenological function $f(p, p', \sigma, \sigma')$ defined² as the second variational derivative of the total energy density of the system with respect to the distribution function. Excepting the term in square brackets, the susceptibility has the well-known form for the susceptibility of a degenerate gas of spin- $\frac{1}{2}$ particles. The term in square brackets results because the average spin of a quasi-particle depends not only on the external field but also, in a self-consistent way through the effective quasi-particle spin interaction, on the average spin of the quasi-particles at the Fermi surface. Hence, there is an effective local field acting on the quasi-particles which differs from the applied field by an amount proportional to the average magnetization. The quantity $(\partial\tau/\partial\epsilon)_\mu$ in Eq. (1) can be evaluated empirically from the specific heat per unit volume, c , which is given by¹²

$$c = \frac{1}{3}\pi^2 k^2 (\partial\tau/\partial\epsilon)_\mu T, \quad (2)$$

where k is the Boltzmann constant.

Application of the theory of Landau to the problem of self-diffusion in He³ has been made by Hone,¹³ who finds that the coefficient of self-diffusion for the magnetization can be written

$$D = \frac{1}{3}V_0^2\tau_D[1 + \frac{1}{4}\bar{\xi}(\partial\tau/\partial\epsilon)_\mu], \quad (3)$$

where V_0 is the velocity of the quasi-particles at the Fermi surface, τ_D is a relaxation time appropriate for diffusion, and the quantity in square brackets is the same one as appears in the formula for the susceptibility, Eq. (1). The quantity $V_0 = P_0/m^*$, where P_0 is the momentum of a quasi-particle at the Fermi surface and m^* is the effective mass, may be obtained from the empirical values of c/R where R is the gas constant, and the number density, N/V , by means of the formulas:

$$P_0 = (3\pi^2\hbar^3 N/V)^{\frac{1}{3}} \quad (4)$$

and

$$m^* = (c\hbar^2/RTk)(3N/\pi V)^{\frac{1}{3}}. \quad (5)$$

The magnetization self-diffusion coefficient given in Eq. (3) has a form similar to that for the self-diffusion of a gas of particles all moving at the same speed but is modified by the term in square brackets which depends explicitly on the spin interaction. This term reduces the self-diffusion coefficient in He³ because the effective spin interaction, which favors parallel spin alignment and, hence, tends to maintain a spin gradient, opposes

⁷ A. C. Anderson, G. Salinger, W. Steyert, and J. C. Wheatley, Phys. Rev. Letters **6**, 331 (1961).

⁸ A. C. Anderson, G. L. Salinger, and J. C. Wheatley, Phys. Rev. Letters **6**, 443 (1961).

⁹ W. R. Abel, A. C. Anderson, and J. C. Wheatley, Phys. Rev. Letters **7**, 299 (1961).

¹⁰ L. D. Landau, J. Exptl. Theoret. Phys. (U.S.S.R.) **32**, 59 (1957); [English translation: Soviet Phys.—JETP **5**, 101 (1957)].

¹¹ L. D. Landau, J. Exptl. Theoret. Phys. (U.S.S.R.) **35**, 97 (1958); [English translation: Soviet Phys.—JETP **8**, 70 (1959)].

¹² A. A. Abrikosov and I. M. Khalatnikov, J. Exptl. Theoret. Phys. (U.S.S.R.) **32**, 1083 (1957); [English translation: Soviet Phys.—JETP **5**, 887 (1957)]; *Reports on Progress in Physics* (The Physical Society, London, 1959), Vol. 22, p. 329.

¹³ D. Hone, Phys. Rev. **121**, 669 (1961).

¹⁴ D. Hone, Phys. Rev. **125**, 1494 (1962).

the natural diffusion of the spins which tends to reduce the spin gradient. The relaxation time for diffusion was derived by Hone and is given by

$$\tau_D = \frac{32\pi^2\hbar^6}{k^2T^2m^{*3}} \left\{ \left[W_D(\theta, \varphi) \frac{(1-\cos\theta)(1-\cos\varphi)}{\cos(\theta/2)} \right]_{av} \right\}^{-1}, \quad (6)$$

where $W_D(\theta, \varphi)$ is the transition probability for the scattering of quasi-particles around the Fermi surface, θ is the angle between the initial momenta of the colliding quasi-particles, and φ is the angle between the planes formed by the initial and final pairs of momentum vectors. From Eqs. (3) and (6), one sees that the diffusion coefficient should have the form

$$D = A/T^2, \quad (7)$$

where A is a parameter independent of temperature but dependent on pressure. The T^{-2} temperature dependence of D reflects the T^{-2} dependence of the collision time. This temperature dependence results, because the number of quasi-particles which can be scattered is restricted to those lying in a region of width kT at the Fermi surface, while the number of final states available is also proportional to kT , the net effect being to make the collision probability per unit time proportional to T^2 .

In our measurements we used the method of spin echoes invented by Hahn¹⁵ in which the motion of the diffusing spins can be followed by means of their relative phases as they precess in a magnetic field with an applied gradient. The elements of the method as used in this experiment are as follows. Consider a system of moments with magnetization in the direction of a static field H_0 in the z direction. Then suppose that a linearly polarized rf magnetic field in the x direction is applied to the system as follows:

$$\begin{aligned} H_x &= 2H_1 \sin\omega_0 t, & 0 \leq t \leq \Lambda \\ H_x &= 0, & t < 0, t > \Lambda \end{aligned} \quad (8)$$

where $\omega_0 = \gamma H_0$. In the laboratory system of reference the moments will nutate with angular frequency γH_1 while the rf field is on. If Λ is long enough to permit many nutation periods, it is possible to measure H_1 by observing the frequency of modulation of the signal at the nutation frequency as observed in a pick-up coil surrounding the sample. In the system of coordinates rotating at angular frequency ω_0 , the magnetization precesses at angular frequency γH_1 in the $y'z'$ plane through an angle of $\gamma H_1 \Lambda$. Of particular importance are those values of Λ for which $\gamma H_1 \Lambda$ is 90° and 180° which define 90° and 180° pulses, respectively.

In our case we apply a 90° pulse; then at a fixed time t_1 later a 180° pulse and then at a variable time $t_2 > 2t_1 + \Delta$ a second 180° pulse. Here Δ is the width of the 90° pulse. During the time that the rf pulses are *not*

on, the field in the z direction is $H_0 + Gz$, where G is a uniform field gradient. Under these conditions one sees two echoes, one at $2t_1 + \Delta$ and the other at $2t_2 - 2t_1 + \Delta$. The separation between the two echoes is $2(t_2 - t_1) \equiv \tau$ but the time the gradient is on is only $\tau - 2\Delta$. In general the second echo will be smaller than the first as a result of increasing phase incoherence with time due to the irreversible processes of self-diffusion and spin-spin relaxation.

An interpretation of the results of spin-echo measurements has been made by Carr and Purcell¹⁶ on the basis of a random walk model and by Torrey¹⁷ on the basis of the Bloch equations modified by a diffusion term. It was pointed out by Hart¹⁸ that in Torrey's derivation it is not necessary to introduce statistics but only to assume that the magnetization current is proportional to the gradient of excess magnetization over equilibrium. The ratio, R , of the amplitudes of the two echoes is related to the spin-spin relaxation time, T_2 , and to the magnetization self-diffusion coefficient by the equation, valid for our experiment,

$$R = \exp[-(\tau/T_2 + (\gamma^2 G^2 D/12)(\tau - 2\Delta)^3)], \quad (9)$$

where τ has been defined above as the time separation of the echoes and 2Δ is the width of a 180° pulse.

In order to measure the relative nuclear susceptibility, it is necessary to reduce the damping of the echoes due to irreversible effects to a negligible value during the time of the measurement. Only a single 180° pulse following the 90° pulse is necessary, and the height of the echo is directly proportional to the static nuclear magnetization which existed before the 90° pulse. In the present experiment T_2 was sufficiently long and $\langle G^2 \rangle_{\text{residual}}$ sufficiently small to make the measurements possible.

EXPERIMENTAL APPARATUS AND PROCEDURE

A. Electronics and Coils

In this work a small resonance field was used. An available air core Helmholtz pair (circular coils separated by half their diameter) of average diameter of 10 in. providing a resonance field of 26.2 G proved to be satisfactory. Power was supplied to the coils by a Power Designs model 353 AM voltage regulated power supply in series with a Kepco model SC32-1 power supply regulated as a constant current source. The reason for the choice of such a small resonance field was to insure that there would be a small magnetic field at the paramagnetic salts which were used to cool the sample and to determine the temperature. This was necessary so as to obtain the lowest possible temperature and, more importantly, to avoid stray magnetic gradients at the sample to these salts.

¹⁶ H. Y. Carr and E. M. Purcell, Phys. Rev. **94**, 630 (1954).

¹⁷ H. C. Torrey, Phys. Rev. **104**, 563 (1956).

¹⁸ H. R. Hart, Jr., thesis, University of Illinois, 1960 (unpublished).

¹⁵ E. L. Hahn, Phys. Rev. **80**, 580 (1950).

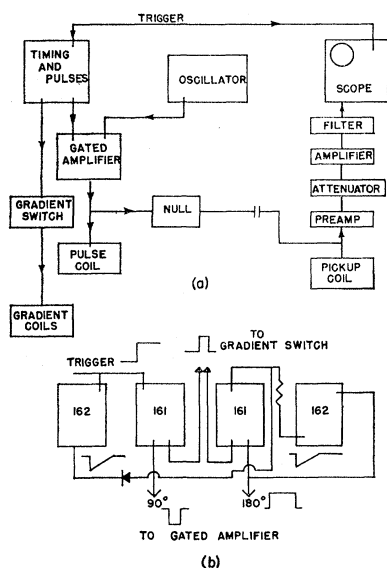


FIG. 1. (a) Block diagram of the spin-echo electronics. (b) Block diagram of the timing and pulse generators. The units are Tektronix 160 series pulse and waveform generators. The diode is a 1N38A. The resistor is 22 k Ω and is chosen so that only two 180° pulses will be delivered.

The gradient was supplied by an air-core Maxwell gradient pair (circular coils separated by $\frac{1}{2}\sqrt{3}$ of their diameter) and was typically about 0.6 G/cm. Since the gradient produced a field inhomogeneity across the sample that was not negligible compared with the resonance field and was the same order of magnitude as the pulse field, the gradient was switched off while the rf pulses were applied. So that the gradient could be switched on an off quickly, the pair was of low-inductance, high-current design. Each coil consisted of 25 turns of number 30 AWG copper wire. The average coil diameter was 4.018 in., the inside spacing between the coils was 3.19 in. and the outside spacing was 3.79 in. To prevent oscillations in the Helmholtz coils when the gradient was switched on and off, counter coils were wound on the Helmholtz pair to cancel the flux through the Helmholtz pair due to the gradient coil. The gradient produced by gradient coils was calculated, correcting for the presence of the counter coils, and the calculated gradient was checked by measuring it with a search coil designed to measure field gradients.

The Helmholtz coils and gradient coils were coaxial and their axis was perpendicular to the cryostat axis.

A block diagram of the electronics employed in the spin echo measurements is shown in Fig. 1(a). The pulse sequence was initiated by a trigger pulse from a manual switch. This signal triggered the oscilloscope and initiated the required pulse sequence by means of the timing and pulse generators which are shown in Fig. 1(b). These consisted of Tektronix 160 series pulse and waveform generators connected as shown. The gate signals from the type-161 units were employed to gate a two-transistor switch which turned off the gradient

current for the duration of an rf pulse. The type-161 units also provided a negative pulse of correct length for the 90° pulse, followed at a fixed time t_1 by a positive pulse of correct length for a 180° pulse, then followed at a variable time t_2 by a second 180° pulse from the same pulse generator. These pulses were converted to the same polarity by a difference amplifier to provide the gate signal which gated on the plate voltage of a two-stage, push-pull, class-A amplifier employing feedback.

The gated amplifier was continuously supplied a signal at the resonance frequency, 85 kc/sec, by a General Radio 805-C signal generator which was transformer coupled to the gated amplifier so as to provide the balanced input required for push-pull operation. Since there was plate voltage on the amplifier only when a pulse was desired, excellent isolation between the oscillator and the pulse coil was obtained.

The output of the gated amplifier was transformer coupled to the pulse coil, a modified Helmholtz pair each half of which consisted of 30 turns of number 30 AWG copper wire, initially in the form of a rectangular loop 5.64 cm long and 3.58 cm wide. The loops were glued symmetrically to a piece of paper which was then formed into a cylinder 3.5 cm in diam, the axis of which was parallel to the long dimension of the loops. The coil then fits on the outside of the glass vacuum case which housed the demagnetization cryostat. The pulse field, $2H_1$, was typically 0.62 G, and was perpendicular both to the field provided by the Helmholtz coils and to the cryostat axis.

The pulse was also fed through an attenuator and phase shifter to the input of the preamplifier in order to null the signal inductively coupled into the pickup coil by the pulse coil. The pickup coil was 1.85 cm long and consisted of 3000 turns of 0.002-in.-diam enamel-insulated manganin wire wound in five sections so as to increase the natural resonant frequency. Manganin was chosen in order to damp any oscillations initiated by the pulses as quickly as possible. This precaution proved to be unnecessary, and a copper pickup coil might have been better.

The preamplifier was of wide-band, low-noise, cascode design and had a gain of approx 40. It was battery powered. The signal was passed through an attenuator to allow a convenient final signal to be selected and then through a wide-band, feedback amplifier having a gain of approx 1000. In order to improve the signal-to-noise ratio the signal was then passed through a tuned filter having a Q of approx 50.

Since we were using a small resonance field and hence a low-resonance frequency, the signal-to-noise ratio was only 15 under the best conditions without enhancement (highest pressure and lowest temperature). In order to improve the signal-to-noise ratio the sample was magnetized in an enhancing field of 100 G which was turned off immediately before initiating the pulse sequence in a time short compared with T_1 , the spin-lattice relaxa-

tion time, but long compared with the Larmor frequency. Under such a scheme the initial magnetization, and hence the signal, is enhanced by a factor of about 4. The enhancement field was provided by a split solenoid mounted on the outside of the He^4 Dewar in liquid nitrogen.

The final signal was displayed on a Tektronix type-531 oscilloscope with a type-D plug-in unit. The oscilloscope trace was photographed with a Polaroid camera and the photographs were measured to obtain the data as discussed in Sec. C.

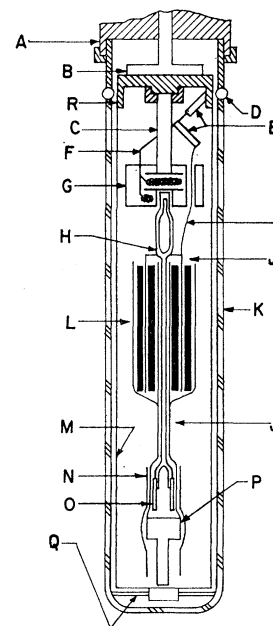
B. Cryogenics

The demagnetization cryostat used in these experiments is shown schematically in Fig. 2. A glass tube, *K*, connected to a copper tube by a Housekeeper seal, *D*, served as a vacuum case to isolate the cryostat from the He^4 bath. It was covered both with a grounded coil-foil¹⁹ which served as an rf shield and with Aquadag and white paper to exclude light. The vacuum case was soldered with Wood's metal to a metal receptacle, *A*, through which all pumping tubes, electrical leads, etc., passed to the experimental space. Receptacle *A* provided adequate light trapping where necessary. *B* is the evaporator of a closed-system He^3 refrigerator capable of cooling the experiment to below 0.3°K . The He^3 refrigerator was connected thermally through lead thermal switches, *E*, to the thermal guard, *G*, and the demagnetization refrigerator, *L*. The lead thermal switches were located in the fringing field of the 12-in. Varian magnet which was used in the demagnetizations and were operated by this field.

The thermal guard was fabricated as follows. A 50-50 mixture by weight of small chromium potassium alum (hereafter called CrK alum) crystals and Epibond 104,²⁰ a catalytic setting epoxy resin, was cast in a Teflon mold in the form of a cylinder 6.3-cm long and 2.3-cm in diameter. A brush of 300 No. 38 AWG copper wires was embedded in the cylinder to provide a path for conducting away the heat of magnetization and to provide a heat sink at the guard temperature. One end of this brush was soldered to a No. 18 AWG copper wire, *F*, to which were soldered the lead switches, *E*. The cylinder was supported by a $\frac{1}{4}$ -in. o.d. \times 0.006-in. wall 70-30 cupro-nickel tube, one end of which was soldered to a copper cap, *R*, which made good mechanical and thermal contact to the evaporator, *B*, of the He^3 refrigerator. The other end of the tube extended 2.5 cm into the guard and was anchored by two copper fins soldered to the tube.

Passing through the guard was a $\frac{1}{8}$ -in. o.d. \times 0.004-in. wall 70-30 cupro-nickel tube through which passed a No. 18 AWG copper wire, *I*, which served as a thermal

FIG. 2. Schematic diagram of the demagnetization cryostat. The parts are identified in the text, but the more important parts include: *B*— He^3 refrigerator evaporator, *E*—lead thermal switches, *G*—thermal guard, *L*—CrK alum refrigerator, *M*—thermal and electrical shield, and *P*— He^3 cell.



link between the CrK alum refrigerator and a lead thermal switch to wire *F*. Wire *I* was insulated over the length passing through the tube with fiberglass sleeving. The CrK alum refrigerator was mechanically supported by a section of thin-wall Pyrex tubing, *H*, which was sealed to a piece of 6-mm Pyrex tubing selected so that it just fit inside a piece of $\frac{1}{4}$ -in. o.d. \times 0.006-in. wall 70-30 cupro-nickel tubing embedded in the bottom of the guard in a manner similar to that of the upper tube described above. The glass tube was glued in with a 50-50 mixture by volume of General Electric 7031 varnish and toluene. The construction of the refrigerator, which contained 37.8 g of CrK alum, and the techniques employed to obtain thermal contact were substantially identical to those fully described elsewhere.¹⁹ Briefly, the refrigerator consisted of alternate layers of CrK alum and coil-foils. The bottom of the CrK alum refrigerator was 8.3 cm from the top of the He^3 cell, *P*. This distance was determined by the requirement that the magnetic field gradient at the sample due to the magnetism of the CrK alum in the field of the Helmholtz pair be less than 0.02 G/cm . This distance was also large enough so that the effect of the CrK alum on the temperature measurements discussed subsequently was negligible.

Thermal contact between the CrK alum refrigerator and the He^3 cell was made by greasing with Apiezon N grease, interleaving, and binding outside a nylon spacer, *O*, the cooling wires extending upwards from the cell with the coil-foils, *J*, extending downwards from the CrK alum refrigerator. The nylon spacer was used so as to keep Pyrex, which is weakly paramagnetic,²¹ away

¹⁹ A. C. Anderson, G. L. Salinger, and J. C. Wheatley, Rev. Sci. Instr. **32**, 1110 (1961).

²⁰ Furane Plastics Inc., 4516 Brazil Street, Los Angeles 39, California.

²¹ G. L. Salinger and J. C. Wheatley, Rev. Sci. Instr. **32**, 872 (1961).

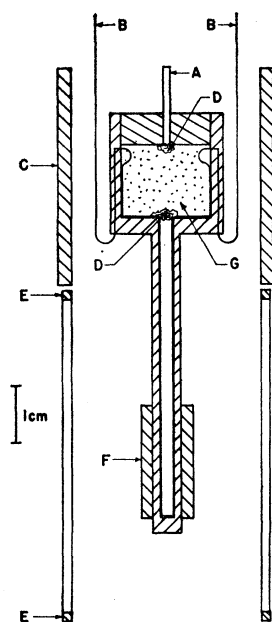


FIG. 3. Scale drawing of the He^3 cell and the associated coils. The parts are as follows: A—cupro-nickel filling tube, B—cooling wires extending to the CrK alum refrigerator, C—mutual inductance set for thermometry, D—cotton filters, E—rf pulse coil set, F—pickup coil, and G—1.29 g of CMN powder.

from the thermometer located in the top of the cell. A cylinder of coil-foil, *N*, thermally connected to the coil-foils, *J*, surrounded the cell and served as a thermal shield. Electrical shielding was provided by the coil-foil shield, *M*, which served primarily as a thermal shield at 0.3°K. This shield was soldered to a copper sleeve which fit closely to the copper cap, *R*, which was in good thermal contact with the evaporation chamber of the He^3 refrigerator. Shield *M* was centered at the bottom by a nylon spacer, *Q*.

A scale drawing of the He^3 cell together with the various coils is shown in Fig. 3. The cell was molded from Epibond 100A,²⁰ a thermal setting epoxy resin, using Teflon forms. The plug which closed the cell was sealed with Epibond 121.²⁰ Both resins are nonmagnetic.²¹

The space containing the He^3 consisted of a cylinder, *G*, 1.2 cm high and 1.2 cm in diam with a coaxial cylindrical tail 5.1 cm long and 0.25 cm in diam. The outside diam of the top cylinder was 1.8 cm while that of the tail was 0.53 cm. The cylinder *G* contained 1.29 g of cerium magnesium nitrate (CMN) powder (grain diam less than 0.015 in.) which served as the thermometer. The whole cell contained 1.0 cm³ of liquid He^3 , but only the He^3 in the bottom 2 cm of the tail was used for the measurements. The inside surface of the cell was lined with 400 insulated, 0.004-in. diam, 99.999% pure copper cooling wires, *B*, about half of which did not extend into the tail. These wires led to the thermal bond to the CrK alum refrigerator which was described above. The cell was filled and pressure applied through a $\frac{1}{4}$ -in. o.d. \times 0.003-in. wall 70-30 cupro-nickel tube, *A*. The CMN was prevented from entering this tube and also from entering the tail by cotton plugs, *D*, which were

glued in place with a 50-50 mixture by volume of General Electric 7031 varnish and toluene.

Coil *F* represents the manganin pickup coil previously described. Coil *E* is a cross section of the rf pulse coil which also has been described previously. This coil produced the linearly polarized pulsed field in a direction perpendicular to the axis of the cell. Coil *C* represents the primary and secondary of a mutual inductance used to measure ballistically the magnetic susceptibility of the CMN. The secondary was wound on a Mylar sheet directly over the primary, and the coil was mounted on the outside of the coil-foil covering the glass vacuum case. Because the rf pulse coil is located in close proximity to the thermometer coils, pulses in the rf coil could excite in the thermometer coils oscillations which then are coupled to the pickup coil causing a spurious signal. To obviate this difficulty the primary, consisting of 1805 turns of No. 38 AWG 99.999% pure copper wire, and the secondary, consisting of 3017 turns of No. 40 AWG copper wire, were both wound with many layers at a high pitch, 25 turns/in. which caused the natural frequency of the coils to be well above the resonance frequency, 85 kc/sec. The primary coil was also made shorter than is usual in this laboratory so that the thermometer coils would not overlap the pulse coils and thus increase the coupling. The total length of the coil set was 3.85 cm, the inside diam was 3.58 cm and the outside diam was 3.84 cm. The resulting configuration proved to be successful.

The cell was designed first to obtain good thermal contact between the He^3 upon which the measurements were being carried out and the CMN thermometer and thus avoid errors in thermometry due to small heat leaks entering between the He^3 and the thermometer, secondly to minimize eddy current heating of the cell due to the rf pulses, and thirdly to locate the CMN sufficiently far from the He^3 sample so that no spurious magnetic gradients would be produced at the sample, which consisted of the He^3 in the final 2 cm of the tail. As a measure of the tight thermal coupling obtained, the thermal time constant between the He^3 and the thermometer was less than 200 sec at all temperatures below 0.1°K. This was fast compared with the thermal time constant of about 1500 sec between the cell and the CrK alum refrigerator for temperatures near 0.05°K.

The thermometry used in this experiment was based on the temperature scale determined in reference 6. In reference 6 the same CMN in the same cell was calibrated by measuring the susceptibility of the CMN in the 4–1°K range and also in the 1–0.3°K range. In the former temperature range it was necessary first to measure the temperature dependent susceptibility of the glass vacuum case and to correct the apparent Curie constant of the thermometer for the presence of the glass. In the latter temperature range as well as in the actual measurements, the glass case is held at a constant temperature. When using such small quanti-

ties of CMN, the temperature dependent magnetism of the glass leads to an appreciable correction. In the 1–0.3°K temperature range the temperature was determined by a 470 Ω Spear resistor which had previously been calibrated with 10 g of CMN. The temperature scale used in reference 6 has an estimated accuracy of 2%. We then calibrated the thermometer used in this experiment by comparing the diffusion coefficient measured at a pressure of 0.17 atm and below 0.1°K with that measured in reference 6. The diffusion coefficient provides a very good method of calibrating a magnetic thermometer in this temperature range, since it changes very rapidly with temperature. This is especially true below about 0.05°K where the diffusion coefficient at this low pressure is known to vary as T^{-2} with considerable accuracy. Based on this calibration procedure and upon the accuracy of the temperature scale used in reference 6, we estimate an accuracy of $\pm 3\%$ for the scale of temperatures used in this experiment. Two such calibrations were carried out, separated by many cycles of the magnetic field, and the calibration constants obtained both times agreed to better than 1%. This agrees with previous experience in this laboratory that, even though CMN is magnetically anisotropic, the powder does not orient itself when placed in a field of 10 000 G, and so is suitable for a thermometer used in a demagnetization experiment. Finally, it should be noted that in the temperature range of this experiment $T^* = T$ for CMN, where T^* is the magnetic temperature of a spherical sample. Our thermometer, which is a cylinder with the diameter equalling the height and a filling factor of about $\frac{1}{2}$, probably has $T^* = T$ within 1%, where T^* is the measured magnetic temperature, even at the lowest temperature.

Pressure was applied to the He^3 through the $\frac{1}{8}$ -in. o.d. cupro-nickel filling tube which was inserted and soldered into a $\frac{1}{32}$ -in. o.d. \times 0.003-in. wall 70-30 cupro-nickel tube which led outside the cryostat. This joint was located near part A of Fig. 2. Pressures were applied by a mercury piston in a stainless steel Toepler pump. The pressure system is shown in Fig. 4. Pressures were measured using a Mansfield and Green dead-weight tester, stated by the manufacturer to be accurate to 0.1%. This unit also served as a manostat. All necessary hydrostatic head corrections were made, an absolute calibration being obtained at low pressures by use of the constant-volume manometer shown in Fig. 4.

C. Experimental Procedure

The cryostat was first cooled to 4°K and the exchange gas pumped out for 15 h. Final degassing was aided by use of an electrical heater mounted on the CrK alum refrigerator. The He^4 pressure was monitored with a Veeco model MS9-A mass spectrometer leak detector. Following pumping out the exchange gas, the bath was pumped to about 1°K, the He^3 refrigerator was started, a magnetic field was applied to turn on the lead thermal

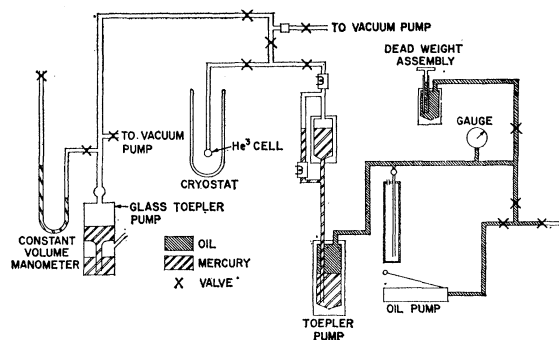


FIG. 4. Schematic diagram of the system used to apply pressure to the He^3 . The He^3 is stored in glass bulbs which are not shown, but connect to the glass Toepler pump.

switches, and the He^3 cell was filled. The leak detector, tuned to the He^3 peak, was used to check for He^3 leaks.

Demagnetizations were carried out as follows. The pressure was set to the desired value and maintained constant during the magnetization and demagnetization using the dead weight tester as a manostat. The magnetic field was increased to 10 600 G. The He^3 refrigerator then cooled the CrK alum refrigerator and associated parts to below 0.4°K, a process which took about 3 h. Then the central field was reduced to a value of 3500 G, which was sufficient to turn off the lead thermal switches which were located in the fringing field of the magnet. The field was then reduced to zero in five equal steps with a pause of approximately 25 min between steps.

The He^3 evaporator had sufficient heat capacity when filled to allow us to increase the pressure of the external He^4 bath to atmospheric pressure and transfer liquid He^4 without appreciable warming of the experiment. This greatly facilitated the running of the experiment by allowing a long running time (days if necessary) on a single demagnetization.

The electronics were tuned using the following procedure. First, all the electronics and magnet supplies were turned on and allowed to stabilize. They were not turned off for the duration of the experiment. An initial demagnetization to about 0.05°K was then performed, since tuning was more convenient at low temperatures because of a larger signal and shorter T_1 . The resonance field was first found by slowly changing the external field and looking for a free induction decay. Final tuning was accomplished by beating the oscillator signal against the free induction decay in zero applied gradient. H_1 was then measured by applying an rf pulse of approximately 30 msec duration and observing the nutation frequency during application of the pulse. For this, the inductive feed-through had to be carefully balanced with the null balance circuit. This enabled us to set the 90° and the 180° pulses accurately. As a further check, no free induction decay was observed following a single 180° pulse.

The self-diffusion coefficient was measured by taking a sequence of six photographs of the echo signal using

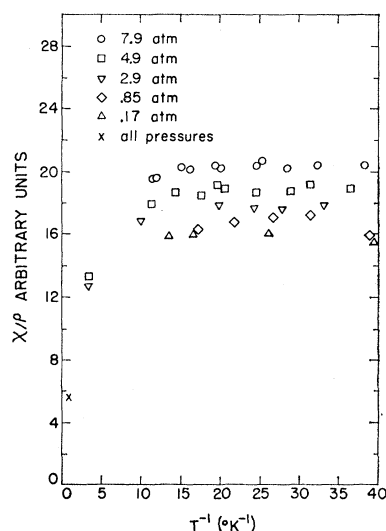


FIG. 5. The nuclear magnetic susceptibility, χ , of He^3 divided by the density, ρ , in arbitrary units between 0.17 atm and 7.9 atm plotted against $1/T$. The points represent the unweighted average of a number of measurements at each temperature and pressure.

different times τ between echoes. Usually, four or more of these sets were taken at a given temperature and pressure with the external gradient in alternate directions so as to eliminate to first order the effects of any residual gradients. The effect due to reversing the gradient was less than 5% and roughly temperature independent. Most probably the residual gradient responsible for this effect was due to the weak temperature independent paramagnetism of the manganin pickup coil.²¹ The photographs were then analyzed by illuminating them from behind and measuring them under a simple magnifying glass with a good quality engineering rule having 0.02-in. divisions in order to obtain the heights of the first and second echoes and their time separation. This method of reading proved to be rapid and was not a limitation on the accuracy of the experimental data. The sweep scale of the oscilloscope was calibrated with a Tektronix time mark generator. The time separation was corrected for the time that the gradient was off during the second 180° pulse. The resulting measurements were fit to Eq. (9), ignoring the effects of T_2 decay. Some crude measurements of T_2 were made by repeating the measurements in zero applied gradient to determine an exponential decay by using such time separations that diffusion in the residual gradients had not appreciably damped the signal. Below 0.1°K , T_2 was about 0.75 sec and at 0.3°K it was 1.75 sec. It was found that within the accuracy of these determinations, about $\pm 25\%$, T_2 was not sensitive to changes in pressure. These values of T_2 have no appreciable effect on our values of D calculated ignoring T_2 effects. It was found, as observed by Garwin and Reich³ and by Hart¹⁸ that the ratio of the echo amplitudes did

TABLE I. The temperature, T_b , at which the diffusion coefficient appears to become proportional to T^{-2} and the ratio $\hbar/\tau_D k T_b$ as functions of pressure.

P (atm)	T_b ($^\circ\text{K}$)	$\hbar/\tau_D(T_b)kT_b$
0.17	0.050	0.84
0.85	0.045	0.74
2.90	0.043	0.93
4.86	0.048	1.26
7.86	0.040	1.10
11.6	0.050	1.42
16.7	0.040	1.20
20.8	0.036	1.19
24.8	0.030	1.16
28.2	0.029	1.27

not always extrapolate to 1, an effect which possibly can be ascribed to imperfect 180° pulses.

Susceptibility was measured by employing a 90° pulse followed by a single 180° pulse applied 2.5 msec later with no external gradient. For pulses between 2.5 and 5 msec after the initial pulse, no decay with time was observed so that it was concluded that the height of the echo represented that of the undamped signal. The gain of the complete amplifying system was measured after each determination of the susceptibility by applying a reference signal from the oscillator through a fixed attenuator to the input of the preamplifier and measuring the output of the complete system on the oscilloscope. The reference signal was also applied to the oscilloscope and measured. The gain of the oscilloscope amplifiers was checked using the calibration signal provided by the oscilloscope. From these measurements we obtained a parameter proportional to the total system gain. The bulk of the approximately 2% variation in the amplifier system gain observed over a 10 day span was attributable to changes in gain of the oscilloscope amplifiers. The susceptibility measurements were also made using the enhancing field so as to increase the signal to noise ratio. The resulting echo heights were corrected for any changes in gain as well as for any changes in enhancing field.

The interval between turning off the enhancing field and initiating the pulse sequence was short compared to T_1 , but no attempt was made to control it. In making the measurements, a check of signal heights as a function of this interval was made for short intervals and no dependence on the interval could be found. Thus, we concluded that any effects of T_1 decay were negligible in these measurements. If they were not, they would be much more important at low temperatures than above 1°K where T_1 is an order of magnitude larger than below 0.1°K . Such an effect would cause our values of the limiting susceptibility to err by being too small in comparison with the higher temperature values.

The usual procedure followed during the measurements was to set a pressure and demagnetize at constant pressure. When the desired temperature was reached, the CrK alum refrigerator was warmed with the electrical heater to the temperature of the He^3 and thermal

equilibrium established. A set of measurements of both diffusion coefficient and susceptibility were then made and the pressure changed. When thermal equilibrium again prevailed, another set of measurements was made. At times, however, we would heat at constant pressure between measurements. Since the measurements at each pressure were taken over the entire duration of the experiment the results should display not only random errors inherent in the measurements but also scatter due to any long term drifts of the equipment. In this connection, the tuning was checked often, particularly while taking susceptibility measurements, by beating the free induction decay against the oscillator.

RESULTS

The results of the susceptibility measurements at various pressures are given in Figs. 5 and 6 in which the raw susceptibility data has been divided by the densities found by extending the densities given by Sherman and Edeskuty²² to low temperatures on the basis of the isobaric thermal expansion data of Rives and Meyer.²³ Each point is the unweighted average of a number of measurements at the same temperature and pressure, a larger number of measurements being taken at the higher temperatures because of a smaller signal to noise ratio. We estimate the accuracy of any of the points to be 3%. About 2% of this uncertainty is due to the noise factor and 1% is due to the measurement of the photographs, chiefly the difficulty of properly assessing the width of the oscilloscope trace.

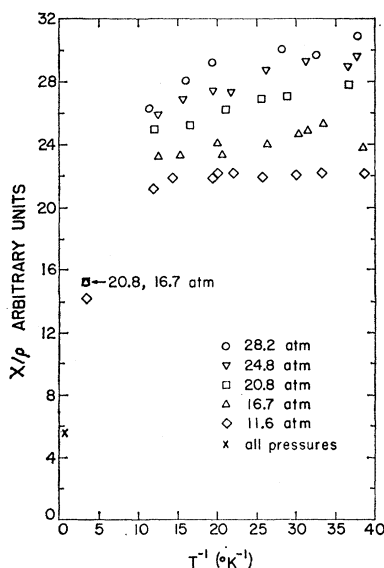


FIG. 6. The nuclear magnetic susceptibility, χ , of He³ divided by the density, ρ , in arbitrary units between 11.6 atm and 28.2 atm plotted against $1/T$. The points represent the unweighted average of a number of measurements at each temperature and pressure.

²² R. H. Sherman and F. J. Edeskuty, Ann. Phys. (New York) **9**, 522 (1960).

²³ J. E. Rives and H. Meyer, Phys. Rev. Letters **7**, 217 (1961).

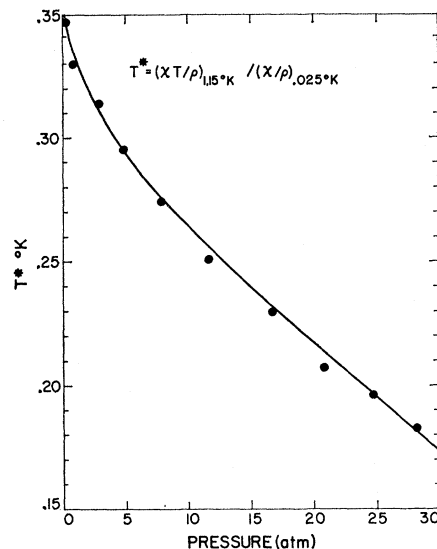


FIG. 7. Effective magnetic temperature, T^* of He³ as a function of pressure. T^* is defined as the ratio of $\chi T/\rho$ taken at 1.15°K to χ/ρ taken at 0.025°K, where χ is the nuclear magnetic susceptibility and ρ is the density.

The susceptibility appears to become temperature independent within the scatter of the experimental data below 0.1°K at 0.17 atm, below about 0.06°K at 0.85 atm, and below temperatures which are nearly the same as those at which the diffusion coefficient becomes proportional to T^{-2} at higher pressures. The latter temperatures are tabulated in Table I.

In Fig. 7 we have plotted an effective magnetic temperature, T^* , defined as the ratio $(\chi T/\rho)_{1.15^\circ\text{K}}/(\chi/\rho)_{0.025^\circ\text{K}}$. This definition of T^* agrees with the usual definition of magnetic temperature in which $T^* \propto \chi/\rho$ and $T^* = T$ above 1°K. Our values of T^* are uniformly 10% higher over the entire range of pressures than the same quantity calculated from the recent results of Thompson and Meyer²⁴ who used a steady-state resonance technique. It should also be noted that our value of T^* at the lowest pressure, 0.17 atm, is $0.349 \pm 0.010^\circ\text{K}$, which agrees within 0.002°K with previous determinations of this quantity in this laboratory.^{5,6} If it is assumed that He³ obeys Curie's law above 1°K and that the limiting low temperature value of the susceptibility has been reached in these experiments, one can evaluate the quantity $[1 + \frac{1}{4}\bar{\epsilon}(\partial\tau/\partial\epsilon)_\mu]$ which occurs in the expression for the susceptibility of a Fermi liquid, and thus one of the parameters of the Landau theory. This quantity is given by the expression

$$1 + \frac{1}{4}\bar{\epsilon}(\partial\tau/\partial\epsilon)_\mu = 3kT^*m^*/P_0^2. \quad (10)$$

This quantity varies monotonically from 0.30 to 0.20 as the pressure varies from 0.17 to 28.2 atm.

Regarding the applicability of Curie's law above 1°K, we found that the values of $\chi T/\rho$ taken as a function

²⁴ A. L. Thomson and H. Meyer, Bull. Am. Phys. Soc. **7**, 76 (1962).

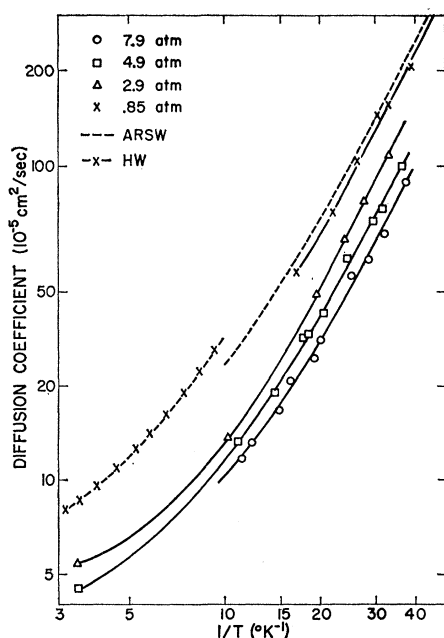


FIG. 8. Self-diffusion coefficient of He^3 plotted against $1/T$. The curves are drawn to have a slope of $1/T^2$ at the low temperature end. The curve labeled ARSW is that of reference 6 taken at 0.17 atm and that labeled HW is that of reference 4 taken at 0.09 atm. The work of reference 4 is known to have inaccuracies in the temperature scale.

of pressure near 1.15°K were constant within 3%, the estimated accuracy of the measurement, and displayed no systematic trend with pressure. Measurements at 2°K proved to be inconclusive because of an adverse signal-to-noise ratio. This constancy with pressure coupled with the sizable variation of T^* with pressure seems to indicate that the susceptibility is not given by the ideal Fermi law and that it is possible that Curie's law may be valid for He^3 at 1.15°K . Thompson and Meyer²⁴ had similar results, finding the susceptibility proportional to the density near 1°K . This conclusion is in accord with the reported measurements of Fairbank, Ard, and Walters¹ above 1°K , although it seems to be inconsistent with their assumed Fermi-Dirac susceptibility law with a degeneracy temperature of 0.45°K for He^3 at the saturated vapor pressure. There appears to be no *a priori* reason to expect that the susceptibility should follow precisely the Fermi-Dirac law. However, if one normalizes our data to an ideal Fermi-Dirac curve, as did they, one obtains an apparent degeneracy temperature of $0.475 \pm 0.010^\circ\text{K}$, in reasonable agreement with reference 1. Comparison with the results of Schwettman and Rorschach²⁵ above 1°K are possibly not valid due to the 10% He^4 content of their sample.

The results of the measurements of the self-diffusion coefficient at various pressures are given in Figs. 8 and

9. The curves have been drawn so that all have a slope of T^{-2} at the lowest temperatures, although at the highest pressures it is not certain that this dependence has yet been reached. The individual points, which are averages of a number of points as previously discussed, have an estimated accuracy of about 3%. Of this, 2% comes from a 1% uncertainty in the value of the field gradient and the other 1% from uncertainties in finding the slope of a $\log R$ vs $(\tau - 2\Delta)^3$ plot, an uncertainty which encompasses uncertainties in the measurements of the heights of the echoes and in the time scale. The results of reference 6 and those of Hart and Wheatley⁴ for the diffusion coefficient at low pressures have been included for comparison. The values of D near 0.3°K agree with a reasonable extrapolation of the 2.4 and the 26.2 atm data of Garwin and Reich.³ The temperature, T_b , where D appears to become proportional to T^{-2} is given in Table I.

Using the most recent empirical values of specific heat,⁷ velocity of sound,⁹ density,^{22,23} and our values of the susceptibility as functions of pressure to evaluate the phenomenological parameters of the Landau theory, we have calculated the theoretical dependence of the self-diffusion coefficient using Eqs. (3) and (6) and Hone's¹⁴ estimate for the form of $W_D(\theta, \phi)$. This predicts that the diffusion coefficient is of the form $D = A/T^2$. Figure 10 compares the theoretical value of A as a function of pressure with the values derived from the experimental measurements by fitting the lowest temperature points to a T^{-2} curve. The absolute accuracy of the experimental coefficient A is about 9% based on the uncertainties of the temperature scale and the measurements of the diffusion coefficient. This is true except

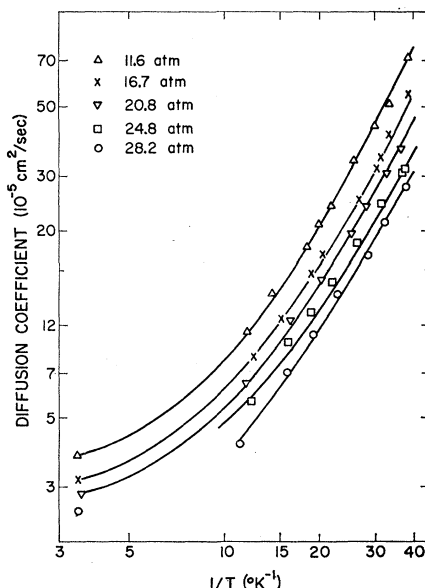


FIG. 9. Self-diffusion coefficient of He^3 plotted against $1/T$. The solid curves are drawn to have a slope of $1/T^2$ at the low temperature end.

²⁵ H. A. Schwettman and H. E. Rorschach, *Proceedings of the Seventh International Conference on Low-Temperature Physics, Toronto, 1960* (University of Toronto Press, Toronto, 1961), p. 604.

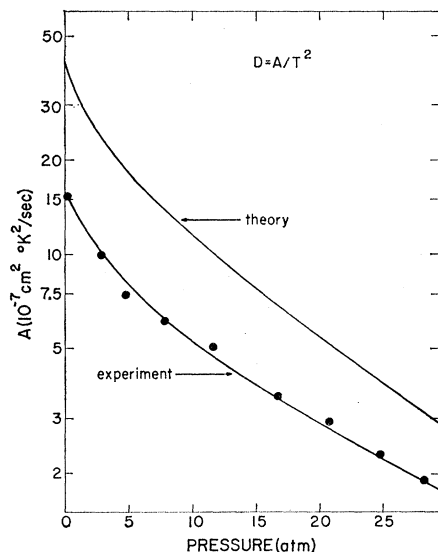


FIG. 10. The coefficient A in the relation $D=A/T^2$, where D is the self-diffusion coefficient, as a function of pressure. The experimental values are taken from the curves of Figs. 8 and 9, while the theoretical values were calculated using the most recent empirical data for the velocity of sound, density, effective mass, and T^* to evaluate Hone's estimate of the form of the scattering probability.

possibly at the highest pressures where A may be somewhat smaller than that taken since the proper temperature dependence may not have been reached. Quantitatively the theoretical curve for A is about twice the measured value, a factor Hone estimates may be the uncertainty of the theoretical expression due to the treatment of the angular average. Since the calculated value of A is quite sensitive to the value of m^* and T^* used, and these cannot be said to be known accurately, especially at the higher pressures, the agreement in

shape of the experimental and theoretical curves may be fortuitous.

Using Eq. (3) we may find the lifetime for diffusion from the experimental data. If we use Eqs. (3), (4), (7), and (10) we find that

$$\tau_D = Am^*/kT^*T^2. \quad (11)$$

We can calculate $\tau_D(T_b)$ at the estimated temperature, T_b , where D appears to become proportional to T^{-2} , and also the ratio

$$\hbar/\tau_D(T_b)kT_b, \quad (12)$$

which is an estimate of the ratio of the energy spread of the quasi-particle states due to collisions to the thermal energy at the temperature T_b . This ratio as a function of pressure is given in Table I. Although T_b is difficult to assess, we have estimated it in a systematic way. Hence, the numerical values of Eq. (12) probably have relative significance, although the absolute values should not be considered definitive. There is considerable scatter, but a criterion such as

$$\hbar/\tau_D(T_b)kT_b \approx 1 \quad (13)$$

seems to determine the boundary of the T^{-2} diffusion region reasonably well.

ACKNOWLEDGMENTS

It is a pleasure to acknowledge many helpful conversations with Professor John Bardeen. Much of the basic electronic gear was assembled by H. R. Hart, Jr. We would like to thank W. R. Abel, J. I. Connolly, E. N. Koch, M. Kuchnir, and R. J. Sarwinski for help in performing the experiment and analyzing data. We would also like to acknowledge several helpful discussions with D. Hone concerning the theoretical evaluation of A .